Latest results from the NA61/SHINE experiment at CERN

Piotr Podlaski

Faculty of Physics, University of Warsaw,
Jan Kochanowski University in Kielce

High Energy Physics Seminar
3.12.2021

NA61/SHINE - UNIQUE MULTIPURPOSE FACILITY:

Hadron production in hadron-nucleus and nucleus-nucleus collisions at high energies

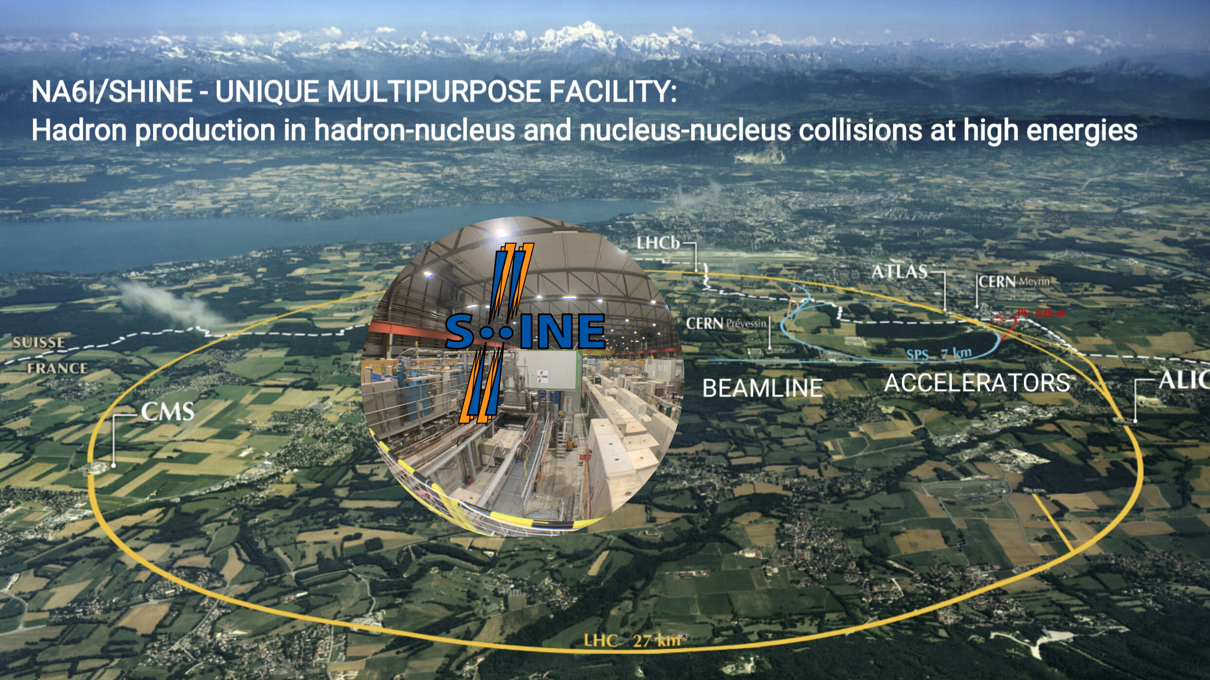

Fixed target experiment located at the CERN SPS accelerator:

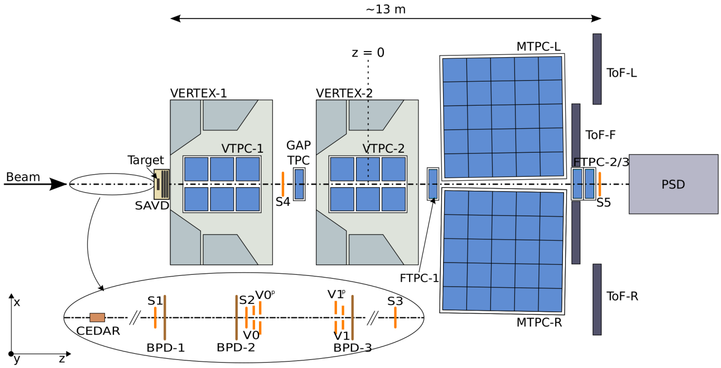

Detector setup includes:

- Set of beam and trigger detectors
- 8 Time Projection Chambers
- 3 Time of Flight detectors
- Hadron calorimeter - Projectile Spectator Detector
- Small Acceptance Vertex Detector

Beams:

- hadrons (π, K, p) p_{beam}=13-400 GeV/c
- ions (Be, Ar, Xe, Pb) p_{beam}=13-150A GeV/c
- $\sqrt{s_{NN}}$=5.1-16.8(27.4) GeV

Large acceptance hadron spectrometer covers the full forward hemisphere, down to $p_T = 0$

Example reconstructed event

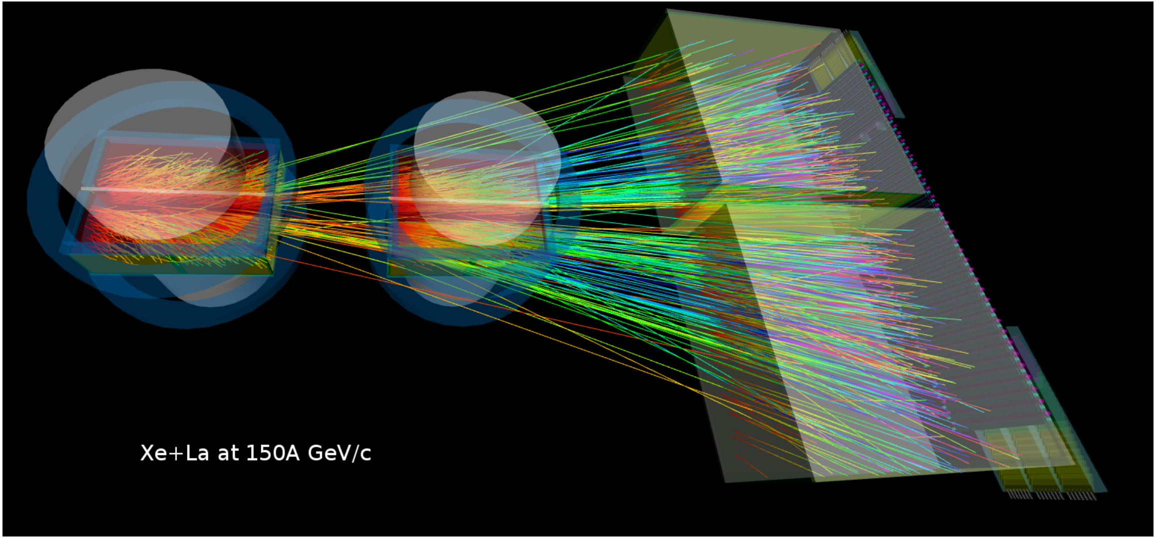

Particle identification

Identification via TPC-measured energy loss, example for Ar+Sc at 150A GeV/c:

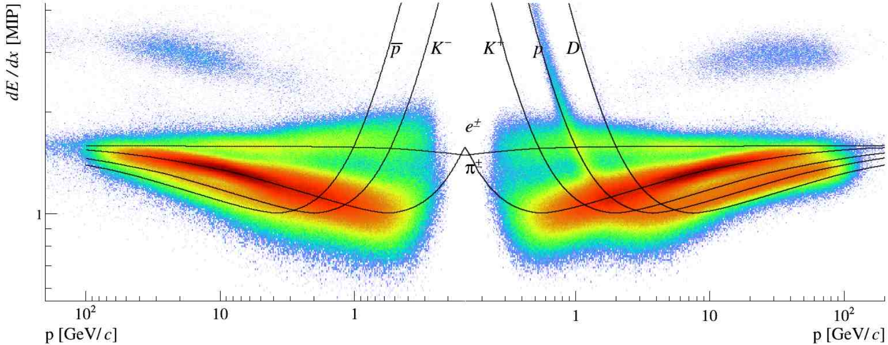

$$\left\langle -\frac{\mathrm{d}E}{\mathrm{d}x} \right\rangle = Kz^2 \frac{Z}{A} \frac{1}{\beta^2} \left[\frac{1}{2} \ln \frac{2m_e c^2 \beta^2 \gamma^2 W_{\max}}{I^2} - \beta^2 - \frac{\delta(\beta\gamma)}{2} \right]$$

Particle identification

Identification via simultaneous measurement of energy loss and time-of-flight, example for Ar+Sc at 30A GeV/c:

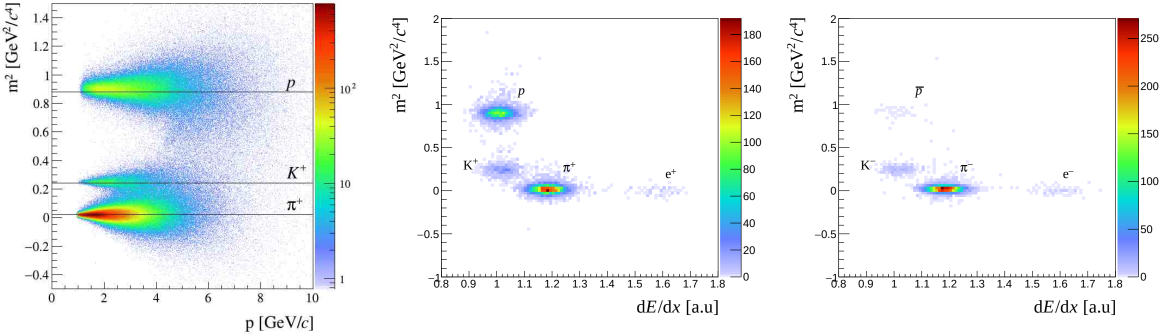

- Excellent particle separation

- Event (centrality) selection in nucleus-nucleus collisions is done using the forward energy(E_F) dominated by energy of projectile spectators and measured by the PSD

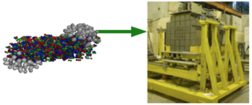

Example of centrality determination for Ar+Sc:

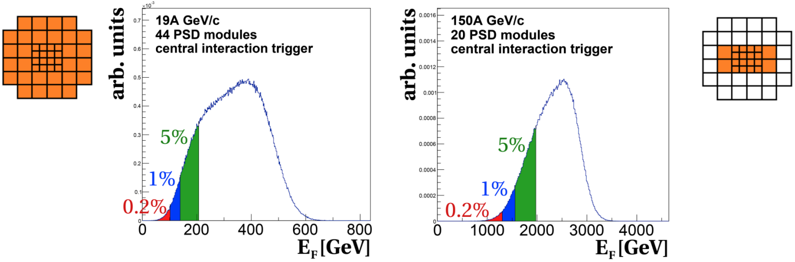

- Selection of modules used for E_F calculation depends on reaction and energy
- Only modules for which energy deposits are dominated by projectile spectators are selected

Strong interaction physics:

- study properties of the **onsets of deconfinement and fireball**
- search for the **critical point** of strongly interacting matter
- direct measurements of **open charm**

Neutrino and cosmic ray physics:

- measurements for neutrino programs at J-PARC and Fermilab
- measurements of nuclear fragmentation cross section for cosmic ray physics

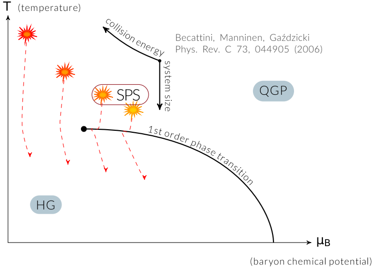

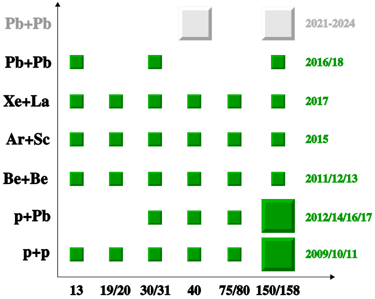

Study of the onset of deconfinement

π^- spectra in Ar+Sc collisions

- Spectra of negatively charged π mesons in Ar+Sc collisions were obtained assuming that majority of negatively charged particles produced in $A + A$ collisions are π^-
- Monte Carlo corrections are applied to take care of the contamination
- Large acceptance (full forward hemisphere, down to $p_T = 0$) allows for calculation of total multiplicity

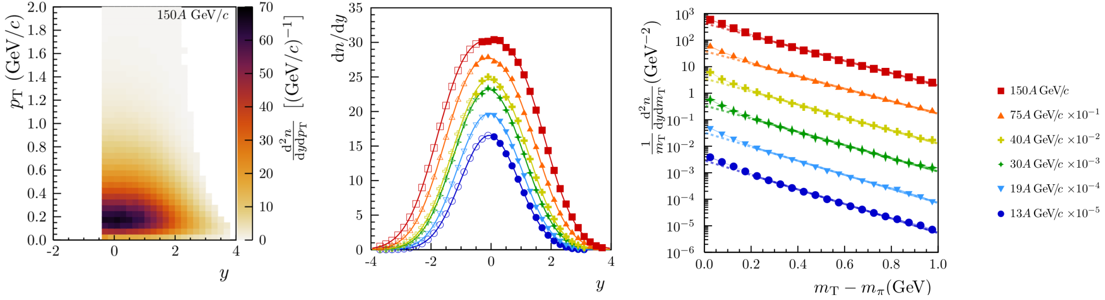

$$m_T = \sqrt{p_T^2/c^2 + m_\pi^2}$$

Eur.Phys.J.C 81 (2021) 5, 397

Onset of deconfinement: kink and dale

Eur.Phys.J.C 81 (2021) 5, 397

$$F = \left[\frac{(\sqrt{s_{NN}} - 2m_N)^3}{\sqrt{s_{NN}}} \right]^{1/4}$$

$$\sigma_y^2(\pi^-) = \frac{8}{3} \frac{c_s^2}{1 - c_s^4} \ln\left(\frac{\sqrt{s_{NN}}}{2m_p} \right)$$

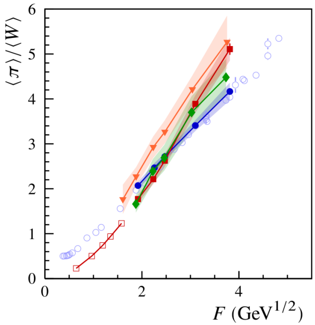

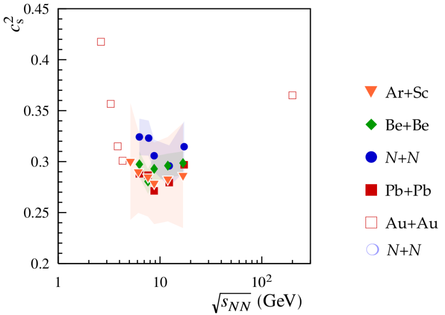

Kink:

- Increase of $\langle \pi^- \rangle / \langle W \rangle$ slope in QGP predicted by statistical model
- $\langle \pi^- \rangle$ per wounded nucleon at SPS energies increases faster in Pb+Pb than p+p
- Ar+Sc slope follows Pb+Pb with systematically higher values

Dale:

- Speed of sound is calculated based on Landau hydrodynamical model
- Energy range for Be+Be and p+p is too limited to allow for conclusion in the presence of the minimum
- Pb+Pb and Ar+Sc exhibit a clear minimum (softest point) at $\sqrt{s_{NN}} \approx 10$ GeV

$K^{\pm}$ spectra in Ar+Sc collisions

K^{+}

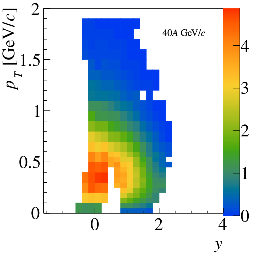

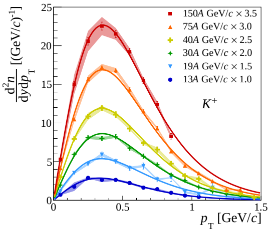

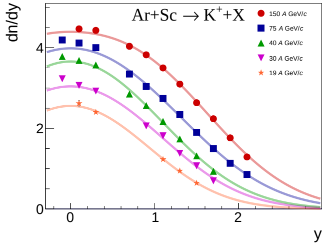

K^{-}

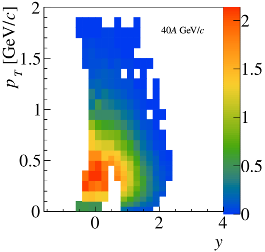

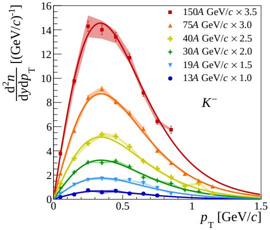

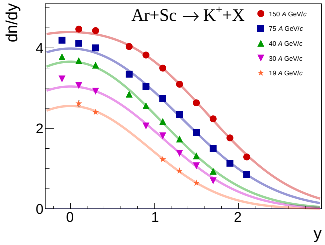

- Inclusive $K^{\pm}$ spectra were obtained with dE/dx and tof-dE/dx analysis methods
- Gap on $y - p_T$ spectrum is caused by difference in acceptances of the two analysis methods

$K^{\pm}$ spectra in Ar+Sc collisions

- In order to obtain the dn/dy yields, the data is extrapolated beyond the detector acceptance
- Exponential dependence in p_T is assumed:

$$f(p_T) = S \cdot p_T \cdot \exp\left(-\frac{\sqrt{p_T^2 + m_K^2} - m_K}{T}\right)$$

- Inverse slope parameter T corresponds to kinetic freezout temperature T_{fo} of the system modified for collective transverse flow during the evolution:

$$T \simeq T_{fo} + \frac{1}{2} m_K \beta_T^2 \tag{1}$$

- To obtain mean multiplicity of produced particles rapidity distribution is fitted with following function:

$$f_{fit}(y) = \frac{A}{\sigma_0\sqrt{2\pi}} exp\left(-\frac{(y-y_0)^2}{2\sigma_0^2}\right) + \frac{A}{\sigma_0\sqrt{2\pi}} exp\left(-\frac{(y+y_0)^2}{2\sigma_0^2}\right)$$

- A, y_0 and σ_0 parameters are fitted

Onset of deconfinement: step

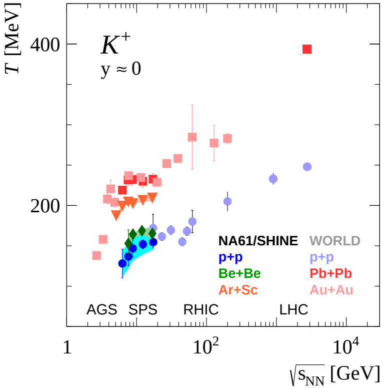

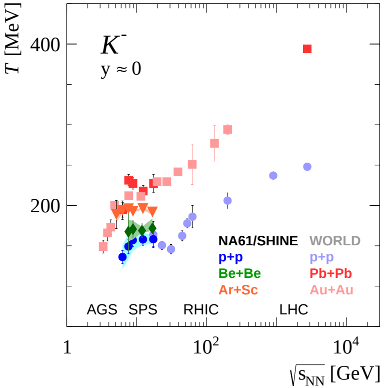

- Plateau in the inverse slope parameter T of m_T spectra of $K^{\pm}$ spectra in Pb+Pb was predicted within SMES due to mixed phase of hadron gas and QGP *Acta Phys. Polon.* **B30**, 2705 (1999)
- Similar structures are visible in other systems
- Magnitude of the T parameter increases with the colliding system size

Onset of deconfinement: horn

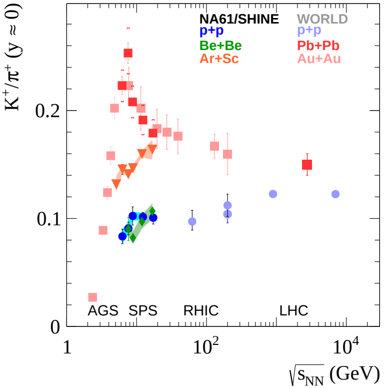

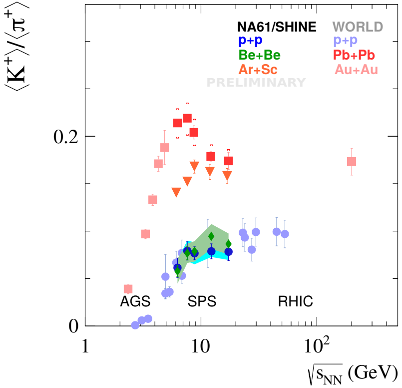

- Rapid change in the energy dependence of K^+/π^+ ratio in Pb+Pb collisions indicated the onset of deconfinement in the SPS energy range, as predicted within SMES
- Plateau like structure visible in small systems (p+p and Be+Be)
- Ar+Sc systematically higher, shows dependence on collision energy qualitatively similar to p+p and Be+Be (no horn structure)

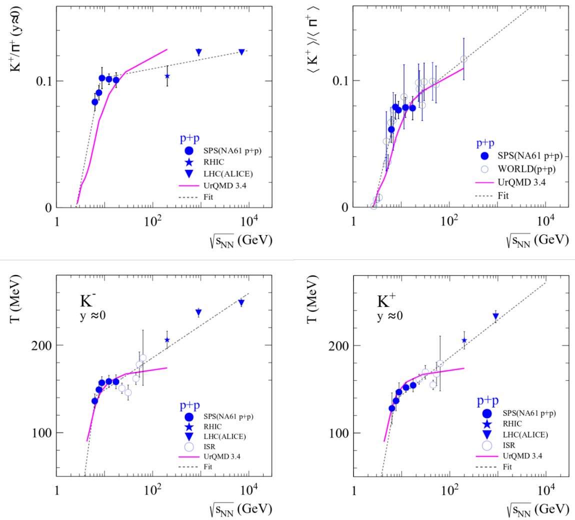

- Rates of increase of K^+/π^+ and T change sharply in p+p collisions at SPS energies
- The fitted change energy is ≈7 GeV - close to the energy of the onset of deconfinement ≈8 GeV
- Models assuming change from resonances to string production mechanism show similar trend

Phys.Rev.C 102 (2020) 1, 011901

Study of the onset of fireball

System size dependence of K^+/π^+ and T at 150A GeV/c

K^+/π^+

dynamical models

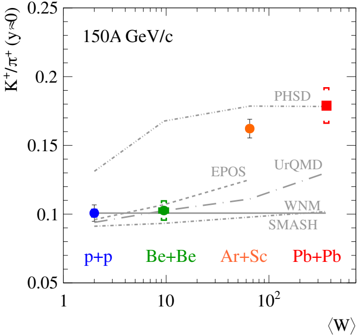

statistical models

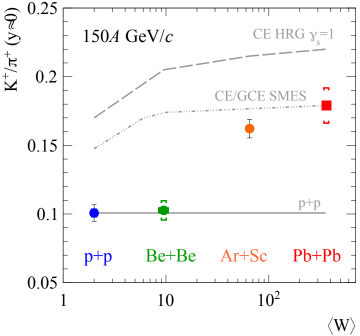

T

dynamical models

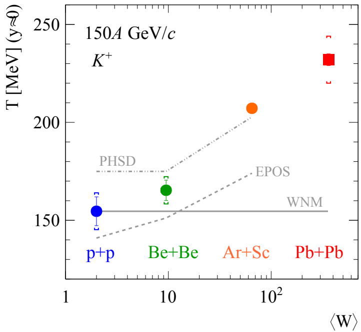

- None of the models reproduce K^+/π^+ ratio or T in the whole $\langle W \rangle$ range

PHSD: Eur.Phys.J.A 56 (2020) 9, 223, arXiv:1908.00451 and private communication;
SMASH: J.Phys.G 47 (2020) 6, 065101 and private communication;
UrQMD and HRG: Phys. Rev. C99 (2019) 3, 034909;
SMES: Acta Phys. Polon. B46 (2015) 10, 1991 - recalculated

p+p: Eur. Phys. J. C77 (2017) 10, 671
Be+Be: Eur. Phys. J. C81 (2021) 1, 73
Ar+Sc: NA61/SHINE preliminary
Pb+Pb: Phys. Rev. C66, 054902 (2002)

Unique NA61/SHINE results on heavy ion collisions

theo: Acta Phys.Polon.B 46 (2015) 10, 1991
exp: Phys.Rev.C 77:024903,(2008)

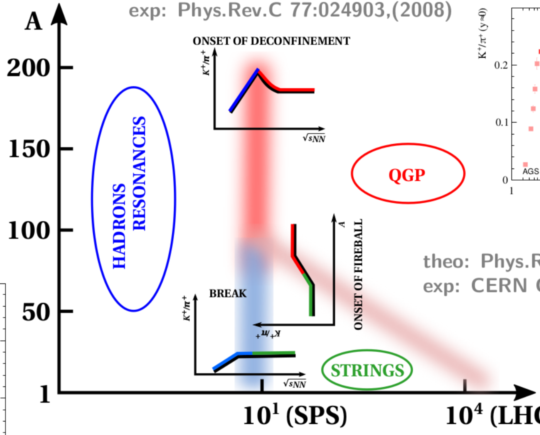

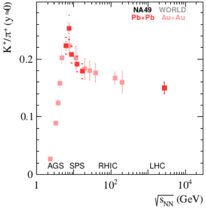

theo: Phys.Rev.D 90 025031 (2014)
exp: CERN Courier, Sep 23^{rd}, 2019

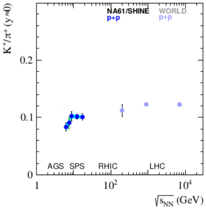

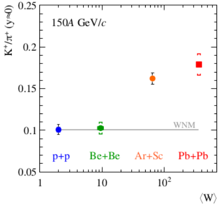

theo: Phys.Part.Nucl. 51 (2020) 3, 337-339
exp: Phys.Rev.C 102 (2020) 1, 011901

Search for Critical Point

Second factorial moment - proton intermittency

Second Scaled Factorial Moment analysis for **primary protons** (strong and electromagnetic processes) produced in Ar+Sc interactions at 150*A* GeV/*c* and Pb+Pb interactions at 30*A* GeV/*c* in few centrality windows using **cumulative variables** and **independent points**.

$$F_2(M) = \frac{\langle \frac{1}{M} \sum_{i=1}^{M} n_i(n_i - 1) \rangle}{\langle \sum_{i=1}^{M} n_i \rangle^2}$$

M - number of p_T subdivision intervals
n_i - number of particles in i-th p_T bin

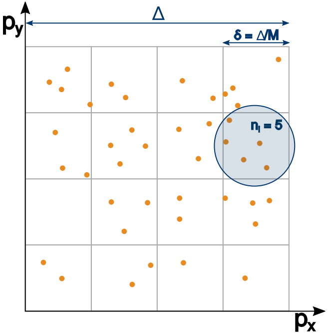

At the second order phase transition $F_2(M)$ exhibits a power-law dependence on M:

$$F_2(M) \sim (M^2)^{\phi_2}$$

Proton intermittency - cumulative variables

Instead of using p_x and p_y, one can use cumulative quantities:

$$Q_x = \int_{x_{min}}^{x} \rho(x)dx \;/ \int_{x_{min}}^{x_{max}} \rho(x)dx \quad Q_y = \int_{y_{min}}^{y} P(x,y)dy \;/P(x)$$

- transform any distribution to uniform one (0,1)
- remove the dependence of F_2 on the shape of the single-particle distribution
- intermittency index of an ideal power-law correlation function system described in two dimensions in momentum space was proven to remain approximately invariant after the transformation

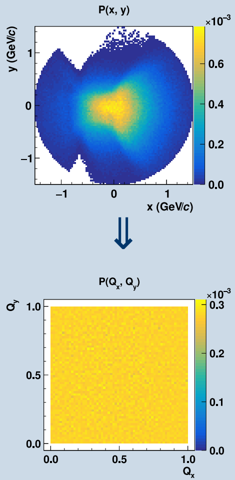

(example for 0-5% Ar+Sc at 150A GeV/c)

PLB 252 (1990) 483

Proton intermittency - results

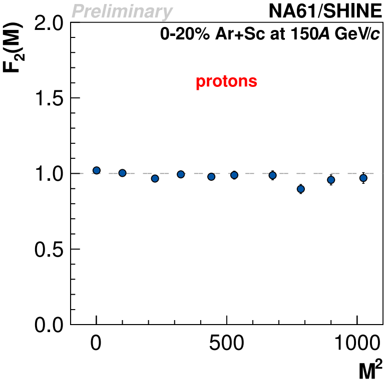

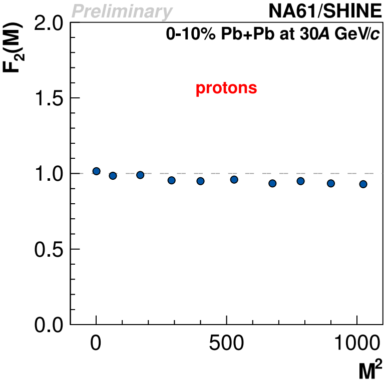

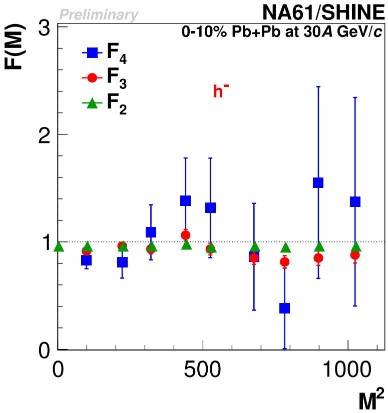

statistical uncertainties only

No indication of power-law increase with bin size

Proton intermittency - simple power-law model

Lots of model data sets generated:

- correlated-to-all ratio: vary from 0.0 to 4.0% (with 0.2 step)
- power-law exponent: vary from 0.00 to 1.00 (with 0.05 step)

and compared with the experimental data

For the construction of exclusion plots, statistical uncertainties were calculated using model with statistics corresponding to the data.

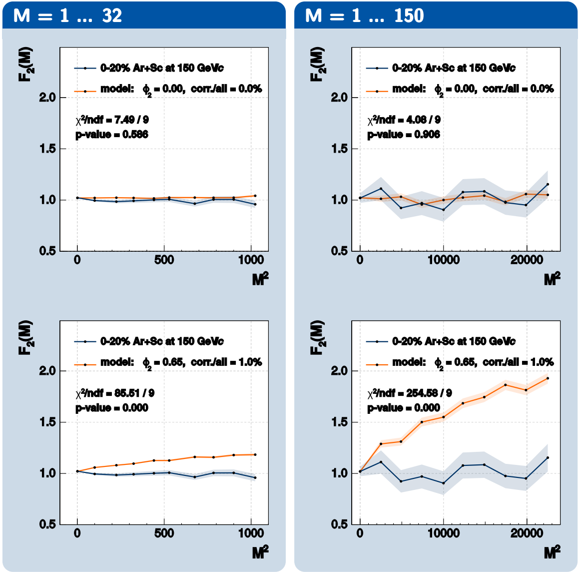

Exclusion plots for parameters of simple power-law model

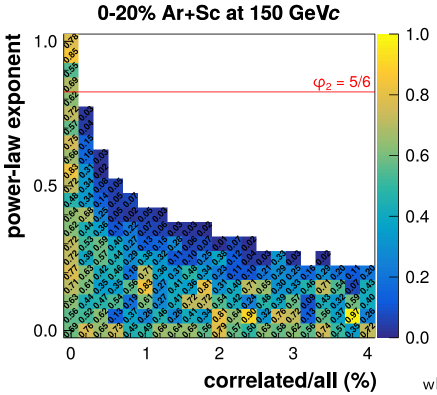

white area:
p-value < 0.01

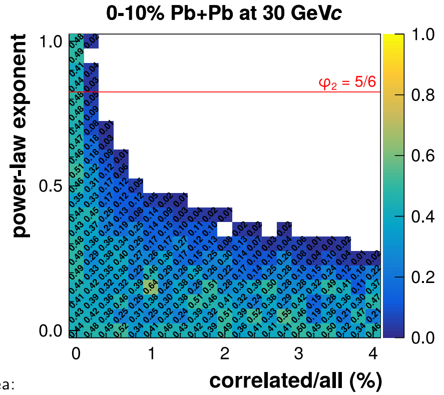

- The intermittency index ϕ_2 for a system freezing out at the QCD critical endpoint is expected to be $\phi_2 = 5/6$ assuming that the latter belongs to the 3-D Ising universality class.

(Multi-)strange hadron production in $p+p$ interactions at $\sqrt{s} = 17.3$ GeV

Ξ^- and $\bar{\Xi}^+$ production

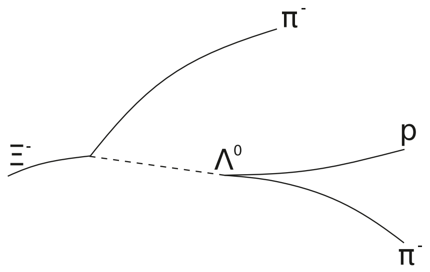

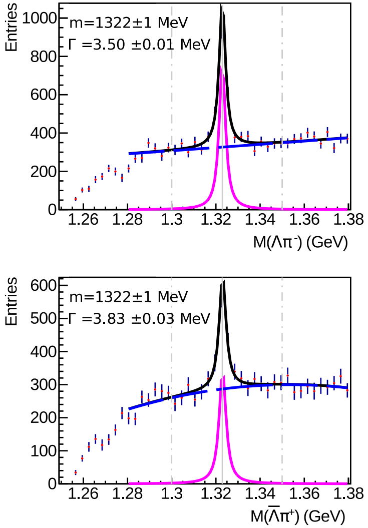

- Reconstruction based on decay topology
- $\Xi^\pm$ decays into $\pi^\pm$ and $\Lambda(\bar{\Lambda})$ with BR≈99.9%
- A set of quality cuts is imposed onto Ξ candidates to improve SNR
- Breit–Wigner function is used to describe signal

Ξ^- and Ξ^+ production

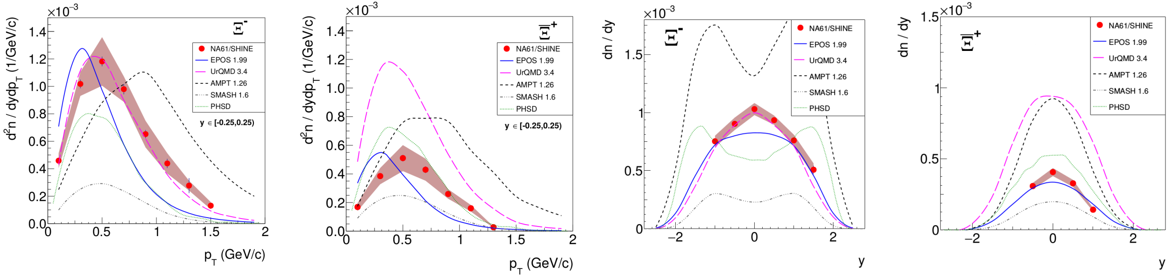

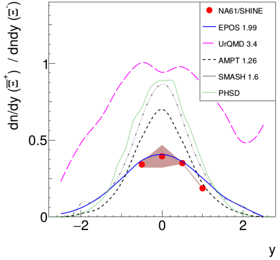

- The only existing results on Ξ^- and Ξ^+ production in SPS energy range
- Strong suppression of Ξ^+: $\langle \Xi^+ \rangle / \langle \Xi^- \rangle = 0.24 \pm 0.01 \pm 0.05$
- Transport models fail to describe the results on Ξ production in p+p collisions

Eur.Phys.J.C 80 (2020) 9, 833

Strangeness enhancement factors

J. Phys. G 32 (2006) 427–442

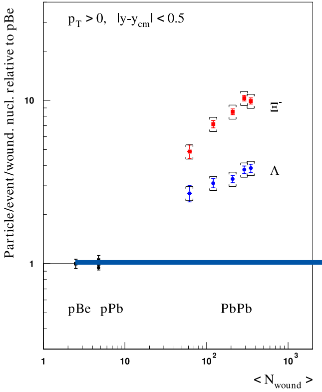

Eur.Phys.J.C 80 (2020) 9, 833

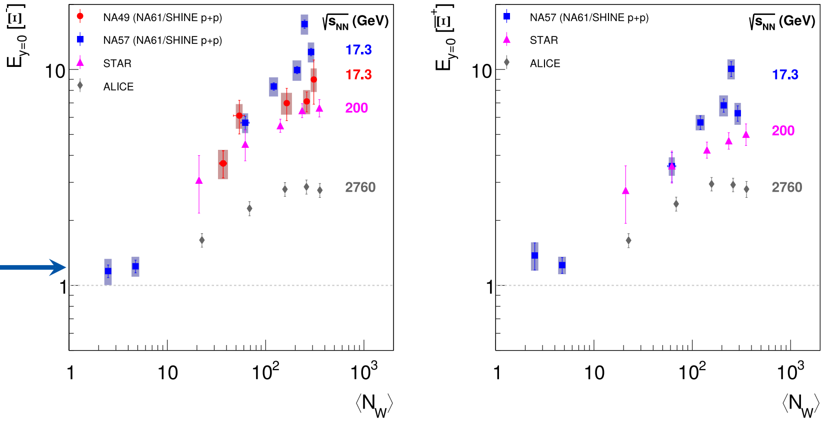

$$E_{\Xi_s} = \frac{2}{\langle W\rangle}\frac{dn/dy(A+A)}{dn/dy(p+p)}$$

NA61/SHINE results give new base-line for strangeness enhancement study in SPS energy range

$\Xi^0(1530)$ and $\bar{\Xi}^0(1530)$ production

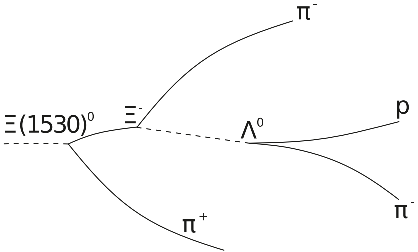

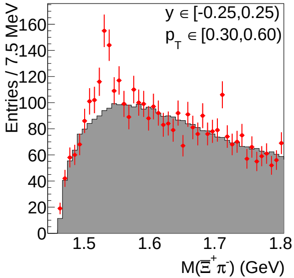

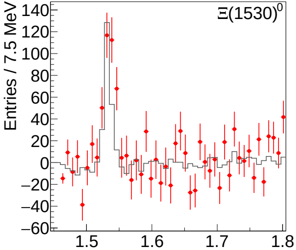

- Reconstruction based on decay topology
- $\Xi^0(1530)$ decays into Ξ and π exclusively
- A set of quality cuts is imposed onto Ξ candidates to improve SNR
- Breit–Wigner function is used to describe signal

$\Xi^0(1530)$ and $\overline{\Xi}^0(1530)$ production

Eur.Phys.J.C 81 (2021) 10, 911

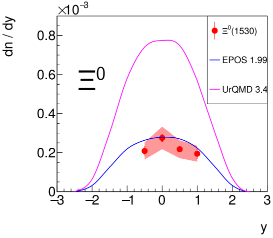

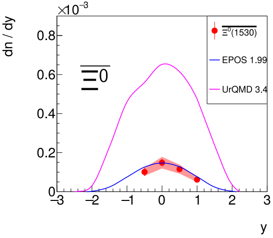

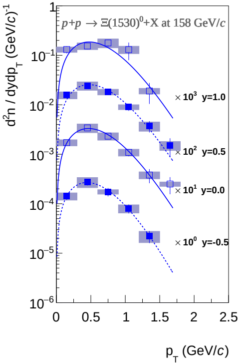

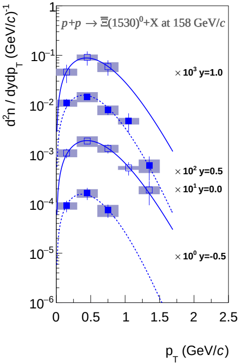

- The first results on $\overline{\Xi}^0(1530)$ production in p+p in SPS energy range
- The second result results on $\Xi^0(1530)$ production in p+p (other measurement was provided by ALICE at 7 TeV Eur.Phys.J.C 75 (2015) 1)
- Suppression of $\overline{\Xi}^0(1530)$: $\langle\overline{\Xi}^0(1530)\rangle / \langle\Xi^0(1530)\rangle \approx 0.40 \pm 0.03 \pm 0.05$

HRG model and $p+p$ data

Eur.Phys.J.C 81 (2021) 10, 911

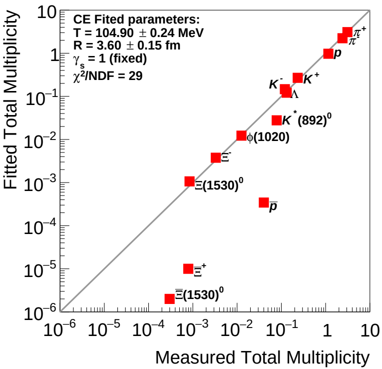

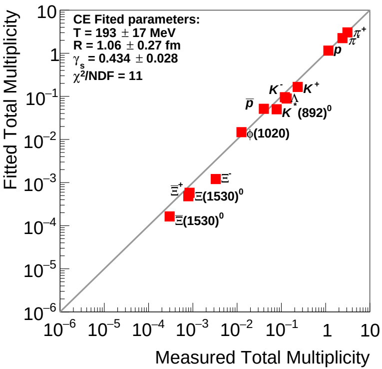

Fit done with different variants of HRG (THERMAL_FIST1.3):

- Canonical Ensemble with fixed $\gamma_s = 1$
- Cannonical Ensemble with fitted γ_s

- Statistical model fails when strangeness saturation parameter γ_s is fixed
- The fit with free γ_s finds $\gamma_s = 0.434 \pm 0.028$
- $p+p$ data are well reproduced by HRG with suppression of strange particles production

$K^*(892)^0$ meson production in $p+p$ interactions at 158 GeV/c

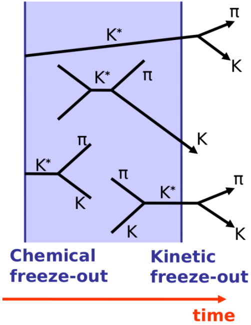

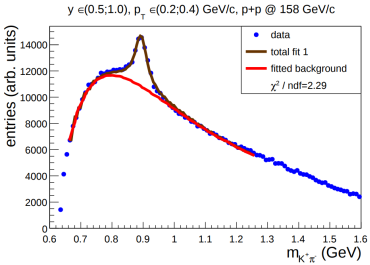

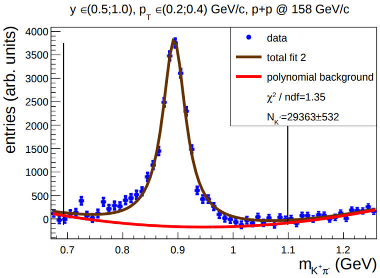

- $K^*(892)^0$ was reconstructed in $K^* \to K^+ + \pi^-$ channel
- The resonance yield is affected by regeneration and rescattering processes
- We have observable sensitive to time between chemical and kinetic freezouts Δt:

$$\frac{K^*}{K^\pm}\bigg|_{kinetic} = \frac{K^*}{K^\pm}\bigg|_{chemical} \cdot e^{-\Delta t/\tau}, \qquad \tau = 4.17\ \mathrm{fm}/c$$

$K^*(892)^0$ meson production in $p+p$ interactions at 158 GeV/c

Eur.Phys.J.C 80 (2020) 5, 460

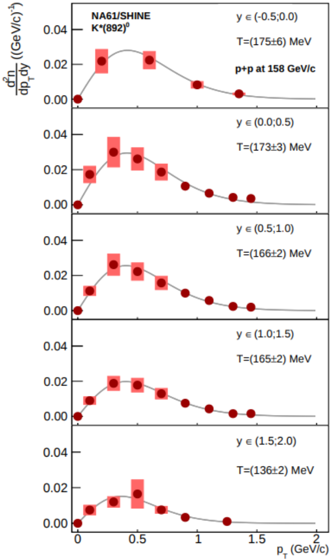

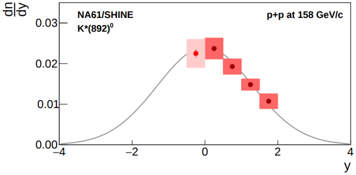

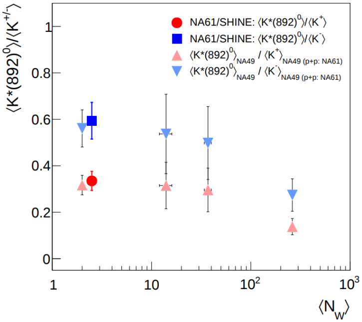

- **Results on $K^*(892)^0$ mass and width were included in PDG**
- time between frezzouts estimated to be $\Delta t \approx 5.3 fm/c$
- $\Delta t_{\mathrm{SPS}} > \Delta t_{\mathrm{RHIC}} \rightarrow$ lifetime of hadronic phase longer at SPS and/or regeneration more important at RHIC energies

Measurements for neutrino and cosmic ray communities

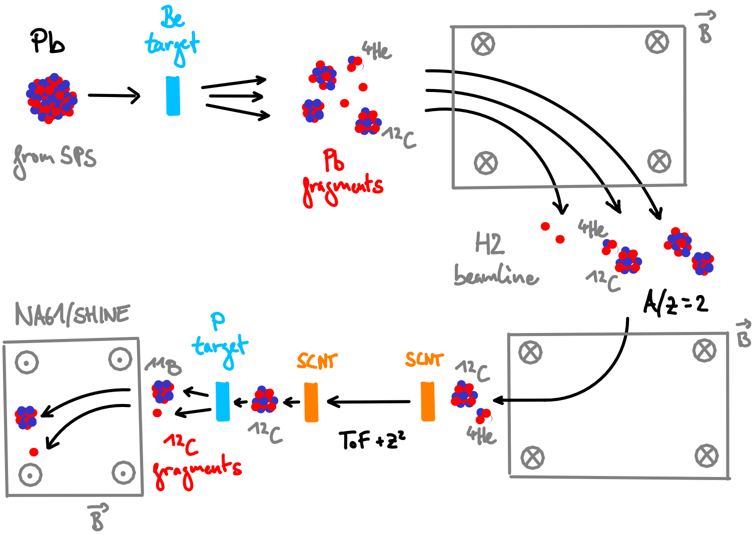

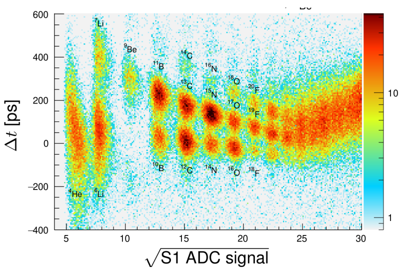

- Goal: measure fragmentation of ^{12}C on protons using polyethylene target
- Pilot run to test feasibility of the method

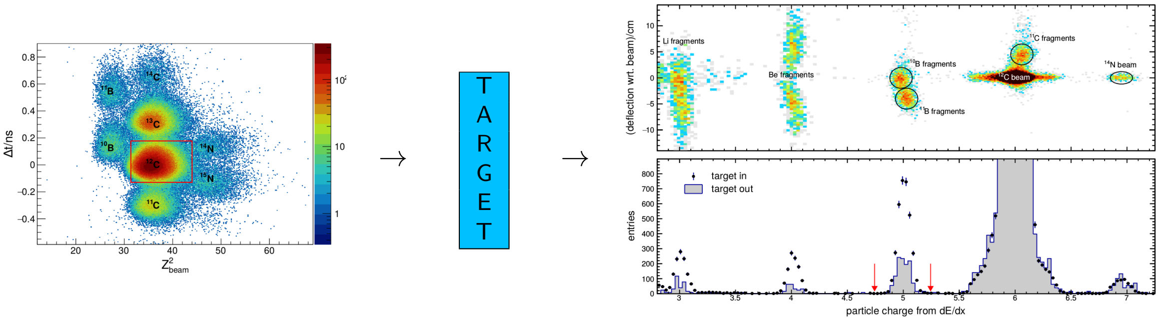

- ^{12}C beam purity: 99.2%, B contamination: $< 0.1\%$
- Pilot run provided first physics result:

$$\sigma_{\mathrm{C}+p\to\mathrm{B}+\mathrm{X}} = (47.7 \pm 3 \pm 2.3)\ \mathrm{mb}$$

PoS ICRC2019 (2019) 446

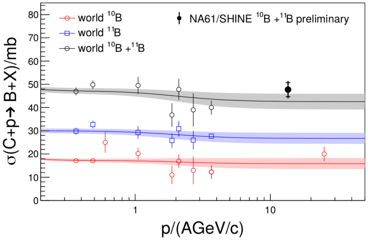

Measurements for neutrino experiment

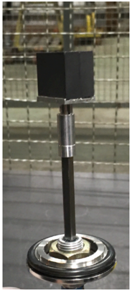

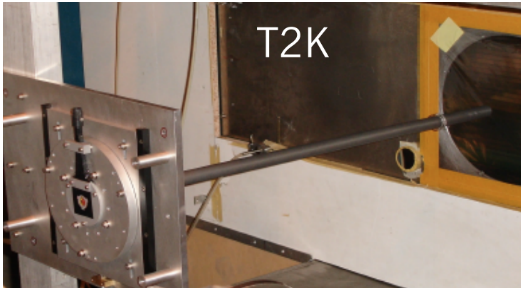

Many measurements for neutrino expetiments (T2K, Numi/NOvA):

- Short target cross sections measurements
- Replica target measurements for precise estimation of neutrino fluxes

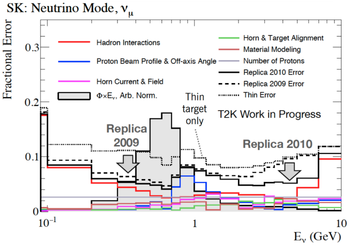

NA61/SHINE in 2022-2024

NA61/SHINE program for 2022-2024

- What is the mechanism of open charm production?
- How does the onset of deconfinement impact open charm production?
- How does the formation of quark-gluon plasma impact J/ψ production?

To answer these questions a **mean number of charm quark pairs**, $\langle c\bar{c}\rangle$, produced in A+A collisions has to be known. Up to now corresponding **experimental data does not exist** and **only NA61/SHINE can perform this measurement in the near future**.

$\langle c\bar{c}\rangle$ and models

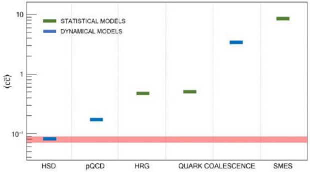

$\langle c\bar{c}\rangle$ and onset of deconfinement

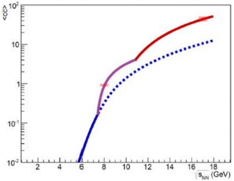

$\langle c\bar{c}\rangle$, $\langle J/\psi\rangle$ and QGP

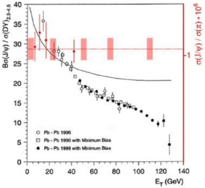

Foreseen NA61/SHINE resolution is sufficient to answer addressed questions

NA61/SHINE detector upgrade - summary

Replacement of the TPC read-out electronics to increase data rate to 1 kHz

Construction of Vertex Detector (VD) for D^0, $\overline{D^0}$ decay reconstruction

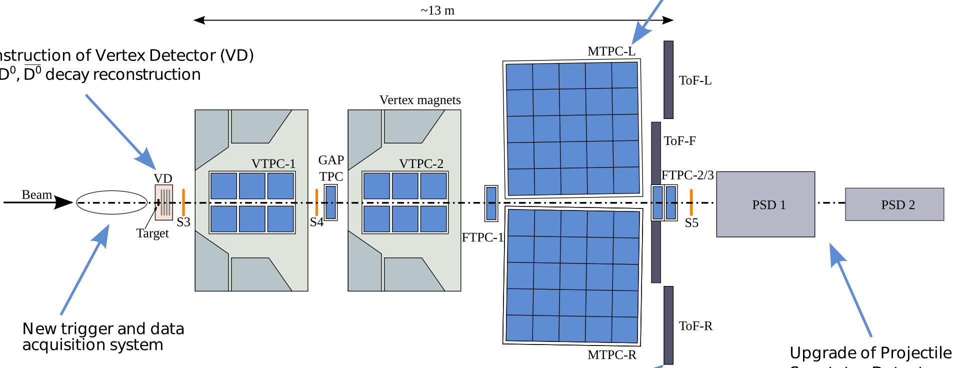

New trigger and data acquisition system

Upgrade of Projectile Spectator Detector

New Time-of-Flight detectors

NA61/SHINE detector upgrade - status

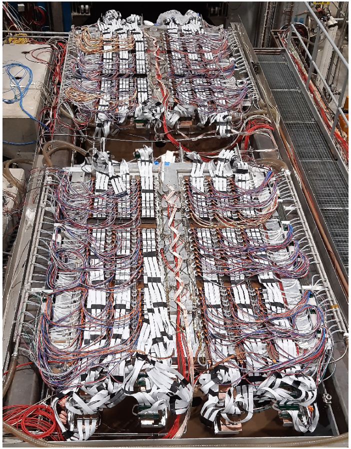

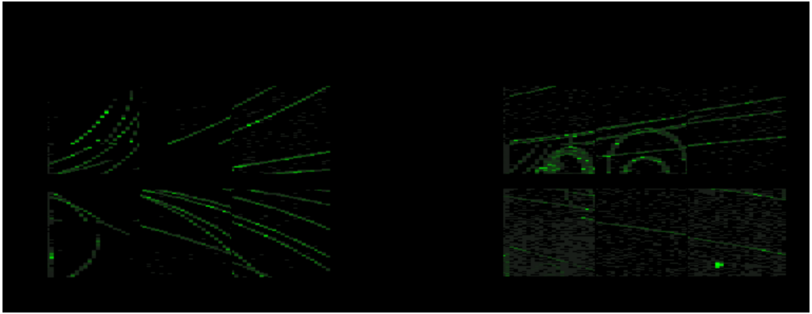

- Installation of electronics on VTPCs completed (September 2021)
- Chambers inserted back into the magnets and tested on beam with full magnetic field (November 2021)

NA61/SHINE detector upgrade - status

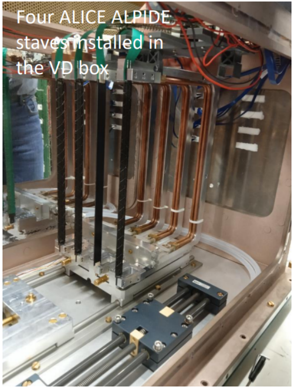

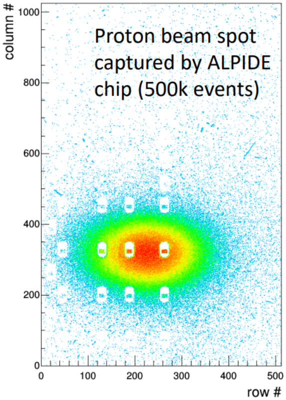

- New mRPC based TOF detector installed and tested (July-November 2021)
- Vertex Detector partially finished and tested on the beam (November 2021)
- Readiness of the upgraded NA61/SHINE detector is foreseen for spring 2022

Summary

- Many new measurements for the study of the onset of deconfinement
- Unexpected system-size dependence: $(p{+}p \approx \mathrm{Be{+}Be}) \neq (\mathrm{Ar{+}Sc} \leqslant \mathrm{Pb{+}Pb})$
- So far no convincing indication of the Critical Point
- Unique results on multi-strange baryons production in $p{+}p$ interactions in SPS
- New fragmentation measurement for cosmic ray physics
- Well defined plan for measurements in 2022-2024
- Hardware upgrade is well advanced: readiness for physics in Spring 2022

Thank you

Backup

Proton intermittency - simple model

A simple model that generates momentum of particles for a given number of events with a given multiplicity distribution.

It has two main parameters:

- ratio of correlated to uncorrelated particles,
- power-law exponent.

Uncorrelated particles (background)

$$\rho_B(p_T) = p_T \cdot e^{-6p_T}$$

Correlated pairs (signal)

$$\rho_S(p_{T,1}, p_{T,2}) = \rho_B(p_{T,1}) \cdot \rho_B(p_{T,2}) \cdot \left[|\Delta p_x|^{\phi} + \epsilon \right]^{-1} \cdot \left[|\Delta p_y|^{\phi} + \epsilon \right]^{-1}$$

Examples for: $\phi = 0.80$
$\epsilon = 1e^{-5}$
N_B=Poisson(30)
N_S=2

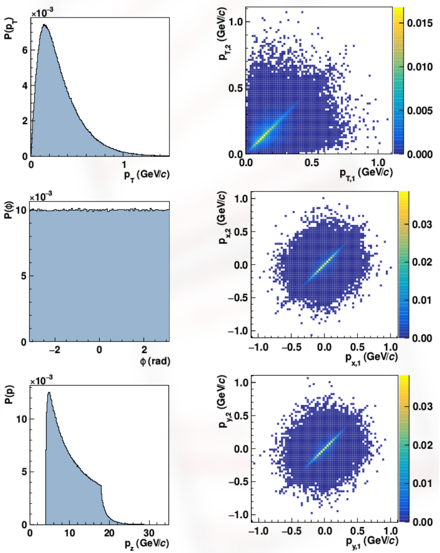

dE/dx and tof-dE/dx acceptance for K^+